

# Superconductivity and Magnetism in $\text{YFe}_2\text{Ge}_2$

David J. Singh

*Materials Science and Technology Division, Oak Ridge National Laboratory, Oak Ridge, Tennessee 37831-6056*

(Dated: September 15, 2021)

We report calculations of the electronic structure and magnetic properties of  $\text{YFe}_2\text{Ge}_2$  and discuss the results in terms of the observed superconductivity near magnetism. We find that  $\text{YFe}_2\text{Ge}_2$  is a material near a magnetic quantum critical point based on comparison of standard density functional results that predict magnetism with experiment. The band structure and Fermi surfaces are very three dimensional and higher conductivity is predicted in the  $c$ -axis direction. The magnetism is of Stoner type and is predominately from an in-plane ferromagnetic tendency. The inter-layer coupling is weak giving a perhaps 2D character to the magnetism, which is in contrast to the conductivity and may be important for suppressing the ordering tendency. This is compatible with a triplet superconducting state mediated by spin fluctuations.

PACS numbers: 74.20.Rp, 74.20.Pq, 74.70.Dd

## I. INTRODUCTION

The interplay of superconductivity and magnetism is a subject of long standing interest.<sup>1</sup> While the early interest was motivated by the observation that nearness to magnetism is destructive to electron-phonon superconductivity, as in e.g. elemental Pd, it was also realized that nearness to magnetism could lead to new forms of unconventional superconductivity with diverse order parameters.<sup>1,2</sup> Such cases can be particularly interesting, as exemplified by the Fe-pnictide and chalcogenide superconductors,<sup>3,4</sup> and perhaps the high  $T_c$  cuprates.<sup>5,6</sup>

The purpose of this paper is to examine the compound  $\text{YFe}_2\text{Ge}_2$ , which was recently found to exhibit superconductivity in close association with a magnetic state.<sup>7</sup>  $\text{YFe}_2\text{Ge}_2$  occurs in the  $\text{ThCr}_2\text{Si}_2$  structure, is based on Fe, and is near to magnetism. This is similar to one of the main families of Fe-based superconductors, specifically doped  $\text{BaFe}_2\text{As}_2$  and related compounds. Unlike those compounds, the specific heat in  $\text{YFe}_2\text{Ge}_2$  appears to be more highly enhanced, the Wilson ratio is higher than two, and the nearby magnetic order is of a different nature than that of the Fe-based superconductors. Several related  $R\text{Fe}_2\text{Ge}_2$  ( $R$ =rare earth) compounds show ordered antiferromagnetism.<sup>8-11</sup> While this has been largely discussed as rare-earth magnetism, the fact that it also occurs in the Lu compound, which has no rare-earth moment indicates that it actually involves the Fe as well.<sup>9</sup> Ishida and co-workers,<sup>12</sup> anticipated a nearness to magnetism early on using density of states arguments, which we confirm in detail here.

## II. APPROACH

Here, we report calculations of the electronic structure and magnetic behavior of  $\text{YFe}_2\text{Ge}_2$  and discuss these in relation to the superconductivity. Our calculations are done within density functional theory, similar to the recently reported work of Subedi.<sup>13</sup> The present calculations were done using the general potential lin-

earized augmented planewave code, with local orbitals,<sup>14</sup> as implemented in the WIEN2k code.<sup>15</sup> We used LAPW sphere radii of 2.5 bohr, 2.2 bohr and 2.2 bohr, for Y, Fe and Ge, respectively. Semicore states (Y 4s, Y 4p, Fe 3p and Ge 3d) were included with the valence states. We used the LAPW plus local orbitals basis set and a well converged planewave cutoff set at  $RK_{max}=9$  (here  $K_{max}$  is the planewave cutoff and  $R$  is the smallest LAPW sphere radius, i.e. 2.2 bohr). The Brillouin zone samplings were done using uniform grids and convergence with respect to these grids was tested. The exchange correlation functional of Perdew, Burke and Ernzerhof (PBE) was employed.<sup>16</sup>

For the structure, we used the experimental lattice parameters of Zou and co-workers, i.e.  $a=3.9617$  Å, and  $c=10.421$  Å; Y at (0,0,0), Fe at (0,1/2,1/4) and (1/2,0,1/4) and Ge at (0,0, $z$ ) and (0,0,1- $z$ ) plus the additional body centered positions  $(x,y,z) \rightarrow (x+1/2,y+1/2,z+1/2)$ . These lattice parameters are similar to those in the earlier experimental report of Venturini and Malaman.<sup>17</sup> The internal coordinate corresponding to the Ge position in the unit cell was determined by total energy minimization. We did this in two ways – non-spin-polarized, corresponding to the experimental paramagnetic state, and spin-polarized in the  $A$ -type antiferromagnetic ground state configuration of the related compounds,  $R\text{Fe}_2\text{Ge}_2$ , which is also the ground state found in the present calculations (see below).

The magnetic calculation yielded  $z=0.373$ , for an Fe-Ge neighbor distance of 2.358 Å, while the non-spin-polarized calculation yielded  $z=0.370$ , for an Fe-Ge neighbor distance of 2.343 Å. This difference indicates a non-negligible magnetoelastic coupling, but still much smaller than the giant effects found in similar calculations for the Fe-based superconductors.<sup>18</sup> The results shown below are for the magnetic value.

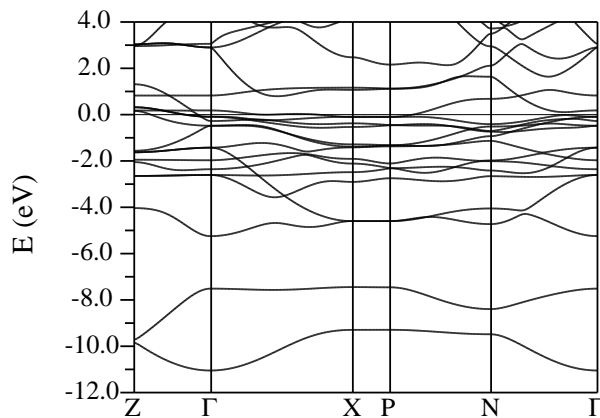


FIG. 1. Band structure of  $\text{YFe}_2\text{Ge}_2$  with the Fermi level at 0 eV. The two deep bands centered at  $\sim -9$  eV are from the Ge 4s state, while the higher valence bands arise primarily from hybridized Ge 4p - Fe 3d states.

### III. ELECTRONIC STRUCTURE

$\text{YFe}_2\text{Ge}_2$  may be notionally related to the iron-superconductors via electron count. Specifically, in comparison to  $\text{SrFe}_2\text{As}_2$ , the replacement of As by Ge and Sr by Y would lead to a deficit of one electron per cell. Then  $\text{YFe}_2\text{Ge}_2$  would be notionally like  $\text{SrFe}_2\text{As}_2$  doped by 0.5 holes per Fe. Interestingly,  $\text{KFe}_2\text{As}_2$ , which has the same electron count, is a low temperature superconductor near magnetism like  $\text{YFe}_2\text{Ge}_2$ .<sup>19</sup>

The band structure and corresponding electronic density of states are shown in Fig. 1 and Fig. 2. The valence band electronic structure derives from hybridized Ge 4p - Fe 3d states, similar to the Fe-pnictide superconductors, and there is dominant Fe 3d character from  $\sim -3$  eV to  $\sim 2$  eV relative to the Fermi energy,  $E_F$ . Similar to hole doped Fe-pnictides, there is a dip in the density of states above  $E_F$  and there is a high  $N(E_F)$ . The calculated value is  $N(E_F) = 5.26 \text{ eV}^{-1}$  on a per formula unit basis. This corresponds to a bare Sommerfeld specific heat coefficient  $\gamma_{\text{bare}} = 12.4 \text{ mJ mol}^{-1} \text{K}^{-2}$ . This is about eight times smaller than the experimental value of  $\gamma \sim 100 \text{ mJ mol}^{-1} \text{K}^{-2}$ . As discussed by Zou and co-workers, such a high value could be due to nearness to a magnetic quantum critical point. Interestingly,  $\text{KFe}_2\text{As}_2$  displays a similarly high value.<sup>20</sup> The Fe *d* contribution to  $N(E_F)$ , as measured by projection onto the Fe LAPW spheres is  $3.99 \text{ eV}^{-1}$  per formula unit, i.e.  $\sim 2 \text{ eV}^{-1}$  per atom, which places the material near Stoner itinerant magnetism. As shown in Fig. 3, this Fe 3d contribution to  $N(E_F)$  comes from multiple orbitals again similar to the Fe-pnictides.<sup>21</sup>

The electronic structure and properties are, however, otherwise very different from those of  $\text{KFe}_2\text{As}_2$ .<sup>22,23</sup> This implies that the physics may also be very different from the Fe-pnictide superconductors.

First of all the electronic structure is very three dimen-

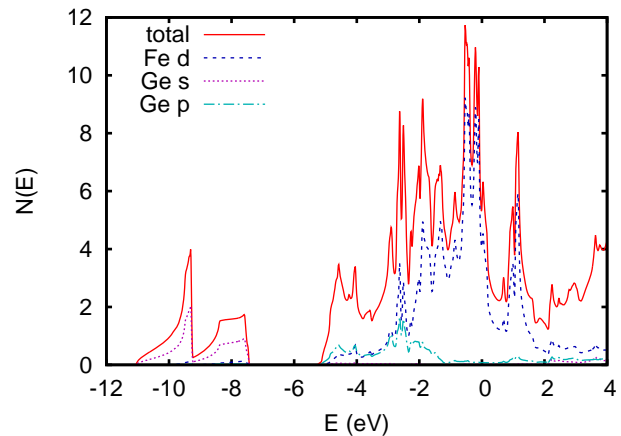


FIG. 2. (color online) Density of states and projections onto LAPW spheres.

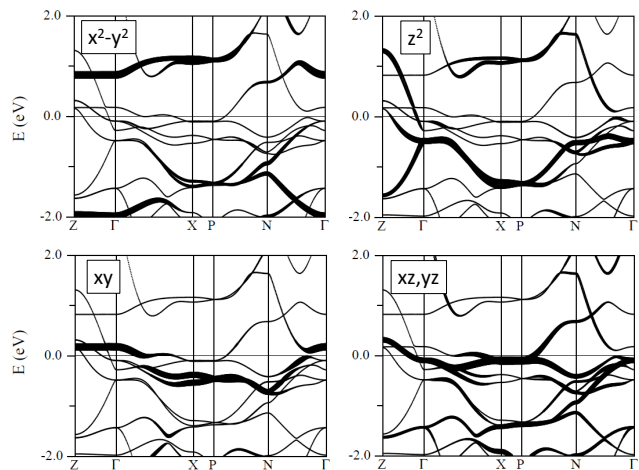


FIG. 3. Band structure of  $\text{YFe}_2\text{Ge}_2$  around the Fermi energy (0 eV, light dotted line), showing the different orbital characters via so-called fat bands plots, in which the size of the plotting points are proportional to the given orbital characters plus a small constant.

sional and has strong dispersion near  $E_F$  in the direction perpendicular to the Fe sheets. As noted by Subedi,<sup>13</sup> the compound has significant Ge-Ge bonding. This can explain the high band dispersion perpendicular to the layers (note that the Shannon ionic radius of trivalent Y is  $1.04 \text{ \AA}$ , i.e. the atom in the layer between the Ge is much smaller than those of the corresponding atoms in the Fe-pnictides, Sr ( $1.32 \text{ \AA}$ ), Ba ( $1.49 \text{ \AA}$ ) or K ( $1.52 \text{ \AA}$ )). The calculated plasma frequencies are  $\hbar\Omega_{p,xx} = \hbar\Omega_{p,yy} = 2.83 \text{ eV}$  and  $\hbar\Omega_{p,zz} = 4.41 \text{ eV}$ . Thus the high conductivity direction is predicted to be perpendicular to the planes, with a sizable anisotropy  $\sigma_{zz}/\sigma_{xx} \sim 2.4$  in the constant scattering time approximation.

The Fermi surfaces are shown in Fig. 4. While there are minor differences from those reported by Subedi,<sup>13</sup> the important aspects are the same. There are three main

sheets of Fermi surface, “3”, “4”, and “5” in Fig. 4, plus several small sheets. The main sheets are a truncated hole cylinder centered at the  $Z$  point, a large disk section that touches the edges of the zone, and electron cylinders at the zone corners. The small surfaces are tiny ellipsoid around  $Z$ , a hole ellipsoid around  $Z$ , and tiny pieces from band extrema near  $E_F$  along  $\Gamma$ - $X$ .

The tiny ellipsoid only  $\sim 0.002$  holes per cell, and is therefore negligible. The second ellipsoid contains 0.08 holes, and the truncated hole cylinder contains 0.15 holes. The electron cylinders at the zone corners have 0.09 electrons and the remainder is the disk. This is the dominant Fermi surface and comes from a near half-filled, but electron doped (filling 1.14 e) band. As seen in the band structure, this comes from a light band of hybridized Fe  $d_{z^2}$  - Ge  $p$  character. The truncated cylinder and the outer ellipsoid have  $d_{xz}, d_{yz}$  character, as do the cylinders at the zone corners. character (here we use a coordinate system where  $z$  is perpendicular to the layers and  $x$  and  $y$  point to the neighboring Fe atoms).

The flat parts of the two larger Fermi surfaces, the truncated cylinder and the disk, are at  $k_z$  of 0.34 and 0.17 of the distance from  $\Gamma$  to  $Z$ , i.e. not at the nesting distance of 0.5 for alternating planes along  $k_z$ . This contradicts the conjecture that the antiferromagnetic ordering tendency of the  $R\text{Fe}_2\text{Ge}_2$  compounds is due to a spin-density wave associated with Fermi surface nesting. In any case, it is clear that the electronic structure and therefore properties of  $\text{YFe}_2\text{Ge}_2$  are dominated by a main disk shaped Fermi surface, which is near half filling but electron doped and is centered around the  $Z$ -point.

#### IV. MAGNETISM

As mentioned, the high  $N(E_F)$  by itself suggests nearness to itinerant magnetism. We do in fact find magnetism in our PBE density functional theory calculations. This magnetism is in contrast to experimental situation, where  $\text{YFe}_2\text{Ge}_2$  is near magnetism, but remains a non-magnetically ordered renormalized paramagnet down to low temperatures. This situation is qualitatively similar to what was found in the Fe-pnictide superconductors, where it indicates nearness to a magnetic quantum critical point.<sup>18,24</sup> In general this type of overestimate of magnetic tendencies within density functional calculations is unusual. It typically arises when spin fluctuations associated with a nearby quantum critical point are strong enough to renormalize the mean-field like magnetic state predicted by standard approximate density functional calculations.<sup>25,26</sup>

The results of fixed spin moment calculations are shown in Fig. 5. As seen there is a sizable ferromagnetic instability, which can be understood as a Stoner instability. This amounts to a spin magnetization of  $1.93 \mu_B$  per cell, consisting of a polarization inside each Fe LAPW sphere of  $1.03 \mu_B$  accompanied by a small back-polarization of the Ge. The magnetic energy is large,

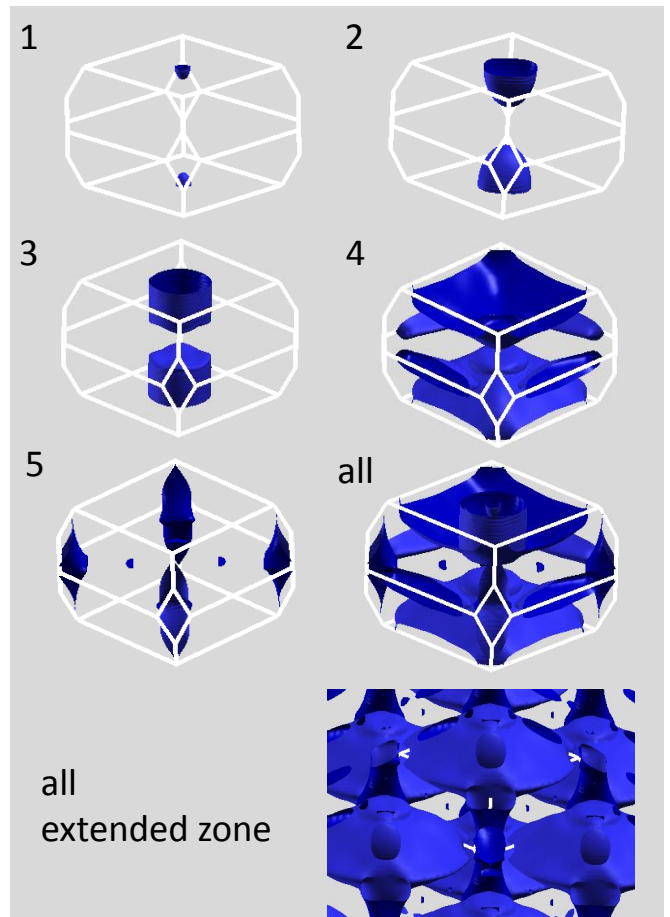


FIG. 4. (color online) Calculated Fermi surfaces of  $\text{YFe}_2\text{Ge}_2$ , showing the five sheets (1-5). The bottom shows the Fermi surface in an extended zone scheme.

$\sim 120$  meV per formula unit. The result is a spin-polarization of the bands, and a lowering of the overall  $N(E_F)$  to  $3.9 \text{ eV}^{-1}$  ( $0.97 \text{ eV}^{-1}$  and  $2.97 \text{ eV}^{-1}$ , for majority and minority spin, respectively).

We also did calculations for other magnetic orders. These were an A-type order, where ferromagnetic Fe planes are stacked antiferromagnetically along the  $c$ -axis direction, a C-type order, where the Fe are arranged in a checkerboard fashion in-plane, and stacked in ferromagnetic chains along  $c$  and a G-type order, with nearest Fe antiferromagnetic both in-plane and along  $c$ . The resulting energies, moments and  $N(E_F)$  are summarized in Table I. As may be seen, the lowest energy state is the A-type, which corresponds to the experimental antiferromagnetic state for  $\text{LuFe}_2\text{Ge}_2$ .

An examination of the energies of the different calculated states shows an itinerant aspect. In particular, the energy differences between the different ordered states are of the same magnitude as the energy differences between the ordered states and the non-spin polarized case, although all the magnetic configurations that we tried do form and have at least slightly lower energy than the non-spin-polarized case. The second apparent feature is that

the A-type and ferromagnetic states are close in energy, while the other two states are also close to each other in energy, but are much above the ferromagnetic state.

Thus the primary driver for magnetism is an in-plane ferromagnetic tendency associated with the high  $N(E_F)$  of the non-spin-polarized state. The interlayer interactions are apparently much weaker as evidenced by the similar energies of the ferromagnetic and A-type ordered states and of the C-type and G-type states. The primary magnetic interactions are in-plane reflecting a layered crystal structure, although the conductivity is predicted to be highest out of plane. Thus  $\text{YFe}_2\text{Ge}_2$  is a very three dimensional metal that nonetheless is predicted to have a more two dimensional magnetic behavior.

It is notable that experimental measurements for the closely related  $\text{LuFe}_2\text{Ge}_2$  compound, which as mentioned is antiferromagnetic, shows Fe moments that lie in the basal plane.<sup>9</sup> This situation with in-plane moments, ferromagnetic interactions in-plane and weak out-of-plane interactions suggests a scenario in which the ordering temperature may be reduced by dimensional effects (specifically, with in plane anisotropy on a square lattice and weak coupling between the planes, one may have a depression of the ordering temperature from that which would be anticipated based on the strength of the in-plane exchange interactions). In this regard, Ferstl and co-workers, who did specific heat and susceptibility measurements for the related compounds  $\text{LuFe}_2\text{Ge}_2$  and  $\text{YbFe}_2\text{Ge}_2$  report evidence for large fluctuating Fe moments high above the ordering temperature.<sup>11</sup> As seen,  $N(E_F)$  is substantially reduced from the non-spin-polarized value by in-plane ferromagnetism (i.e. ferromagnetic and A-type antiferromagnetic order) but not by orders that involve in-plane antiferromagnetism, consistent with the Stoner mechanism. The primarily magnetic tendency that we find is towards in-plane Stoner magnetism, and this, and not a spin-density-wave, is the reason for the moment formation.

In any case, this picture of the magnetism has certain consequences. First of all, one may expect metamagnetic transitions in the  $R\text{Fe}_2\text{Ge}_2$  compounds under high field including the non-magnetic compound  $\text{YFe}_2\text{Ge}_2$ . These may be accompanied by a sizable magnetoresistance, which should be negative in the range where ferromagnetic order becomes imposed by the field. These have been observed in some of the compounds.<sup>10</sup> Secondly, one expects a susceptibility,  $\chi(\mathbf{q})$  that shows weak  $k_z$  dependence and a stronger in-plane dependence peaked near the 2D zone center (and highest at  $Z$ ). As noted by Subedi, there is also a nesting of the small cylinder sheets that can modify this by the addition of a nesting related peak, which would couple the zone center to the zone corner, i.e. an in-plane pattern similar to the Fe-pnictide superconductors, but this would not couple to the main disk shaped Fermi surface.

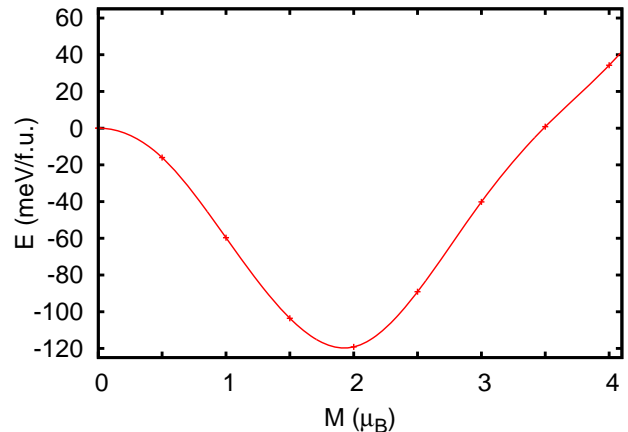


FIG. 5. (color online) Fixed spin moment total energy as a function of constrained spin magnetization for  $\text{YFe}_2\text{Ge}_2$  on a per formula unit basis. The symbols are the calculated points and the curve is a spline interpolation. Note the instability of the non-spin-polarized state against ferromagnetism.

TABLE I. Magnetic energies,  $E$ , moments  $m$  inside the Fe LAPW spheres, radius, 2.2 bohr, and  $N(E_F)$  on a per formula unit basis for different ordering patterns (see text). The energy zero is taken for the non-spin-polarized case, denoted “NSP”.

Order	$m$ ( $\mu_B/\text{Fe}$ )	$E$ (eV/f.u.)	$N(E_F)$ ( $\text{eV}^{-1}$ )
NSP	0.00	0.000	5.3
F	1.03	-0.120	3.9
A	1.04	-0.137	3.6
C	1.26	-0.026	7.0
G	0.98	-0.004	6.4

## V. DISCUSSION

The magnetism has consequences for superconductivity. Almost all superconductors are conventional  $s$ -wave superconductors mediated by electron-phonon interactions, and this may also be the case here. However, there are two features that suggest consideration of other possibilities. First of all, the specific heat  $\gamma$  is very high. This suggests a short coherence length in which case Coulomb avoidance should work against a conventional  $s$ -wave state. Secondly, the nearness to a magnetic quantum critical point with a ferromagnetic character suggests the presence of ferromagnetic spin fluctuations, which are pair breaking for a singlet superconductor. This means that if  $\text{YFe}_2\text{Ge}_2$  is a conventional electron phonon superconductor, it is one in which the superconductivity is heavily affected by magnetism and which would have a considerably higher critical temperature without magnetism.

An alternate scenario to the electron-phonon picture is spin-fluctuation mediated superconductivity. This depends on the interplay between the  $\mathbf{q}$ -dependent spin fluctuations, as characterized by the real part of  $\chi(\mathbf{q})$ , and the Fermi surface. Spin-fluctuations provide a re-

pulsive interaction for singlet superconductivity and an attractive interaction for triplet superconductivity.<sup>1</sup> The resulting superconducting state is then due to matching of the  $\mathbf{q}$  dependence of  $\chi(\mathbf{q})$  with the Fermi surface.

In the present case, the major Fermi surface is the disk around the  $Z$ -point. In a singlet channel one could imagine that spin-fluctuations associated with the antiferromagnetic order (i.e. the antiferromagnetic interaction along the  $c$ -axis) could couple the two faces of the disk. In that case, since one has a repulsive interaction, a state in which the two faces have opposite order parameter would be favored. However, because of the symmetry of the  $Z$  point this would lead to odd parity, i.e. not a singlet, while in a triplet channel the argument works in reverse – the antiferromagnetic tendency would favor having the same sign order parameter on the two faces, which would then have even parity and not be a triplet. Therefore we conclude that the antiferromagnetic interaction along  $c$  is not effective in providing pairing. In any case, as shown by the energies in Table I, this interaction is not particularly strong.

Ferromagnetic spin fluctuations are pair breaking for singlet superconductivity, since they imply a repulsive interaction at low  $\mathbf{q}$  for a singlet. In the triplet case they are attractive at low  $\mathbf{q}$  and superconductivity can arise if the susceptibility falls off on the scale of the Fermi surface size. In the present case, the disk Fermi surface is large, and so it can be anticipated that a triplet state in which the order parameter changes sign going around the Fermi surface will be stabilized. This could be of the  $p$ -wave type proposed for  $\text{Sr}_2\text{RuO}_4$ ,<sup>27,28</sup> which in this case would be a vector order parameter rotating as one goes around periphery of the disk, or perhaps a more complicated triplet state.

## VI. SUMMARY AND CONCLUSIONS

Thus we find that  $\text{YFe}_2\text{Ge}_2$  is a material near a magnetic quantum critical point based on comparison of stan-

dard density functional results that predict magnetism with experiment. The band structure and Fermi surfaces are very three dimensional and higher conductivity is predicted in the  $c$ -axis direction. The magnetism is of Stoner type and is predominately from an in-plane ferromagnetic tendency. The inter-layer coupling is weak giving a perhaps 2D character to the magnetism, which is in contrast to the conductivity and may be important for suppressing the ordering tendency. Based on matching of the Fermi surface with the magnetic tendency, it seems most likely that  $\text{YFe}_2\text{Ge}_2$  is either an electron-phonon superconductor, in which case superconductivity must be strongly suppressed by the magnetic tendency, or a triplet superconductor mediated by the near ferromagnetic spin fluctuations acting on the large Fermi surface. Considering the heavy mass implied by specific heat measurements, the strong mass renormalization, the experimental  $R_W > 2$ , and the very close proximity to ferromagnetism, it seems that the triplet scenario may be realized. Experiments that can distinguish these cases are (1) correlating the critical temperature  $T_c$  with the mean free path when limited by paramagnetic impurities, i.e. inverse correlations between resistivity and  $T_c$ ; (2) Specific heat measurements, since with the complex three dimensional Fermi surface of  $\text{YFe}_2\text{Ge}_2$  a triplet state may not be fully gapped; (3) Spin susceptibility below  $T_c$ , e.g. using Knight shift; and (4) searches for time reversal symmetry breaking.<sup>29,30</sup>

## ACKNOWLEDGMENTS

This work was supported by the U.S. Department of Energy, Basic Energy Sciences, Materials Sciences and Engineering Division.

- 
- <sup>1</sup> N. F. Berk and J. R. Schrieffer, Phys. Rev. Lett. **17**, 433 (1966).
  - <sup>2</sup> N. D. Mathur, F. M. Grosche, S. R. Julian, I. R. Walker, D. M. Freye, R. K. W. Haselwimmer, and G. G. Lonzarich, Nature **394**, 39 (1998).
  - <sup>3</sup> I. I. Mazin, D. J. Singh, M. D. Johannes, and M. H. Du, Phys. Rev. Lett. **101**, 057003 (2008).
  - <sup>4</sup> K. Kuroki, S. Onari, R. Arita, H. Usui, Y. Tanaka, H. Kontani, and H. Aoki, Phys. Rev. Lett. **101**, 087004 (2008).
  - <sup>5</sup> D. J. Scalapino, E. Loh, and J. E. Hirsch, Phys. Rev. B **34**, 8190 (1986).
  - <sup>6</sup> J. R. Schrieffer, X. G. Wen, and S. C. Zhang, Phys. Rev. B **39**, 11663 (1989).
  - <sup>7</sup> Y. Zou, Z. Feng, P. W. Legg, J. Chen, G. I. Lampronti, and F. M. Grosche, cond-mat , arXiv:1311.0247 (2013).

- <sup>8</sup> H. Pinto, M. Melamud, M. Kuznietz, and H. Shaked, Phys. Rev. B **31**, 508 (1985).
- <sup>9</sup> T. Fujiwara, N. Aso, H. Yamamoto, M. Hedo, Y. Saiga, M. Nishi, Y. Uwatoko, and K. Hirota, J. Phys. Soc. Jpn. **76**, SA60 (2007).
- <sup>10</sup> M. A. Avila, S. L. Budko, and P. C. Canfield, J. Magn. Magn. Mater. **270**, 51 (2004).
- <sup>11</sup> J. Ferstl, H. Rosner, and C. Geibel, Physica B **378-380**, 744 (2006).
- <sup>12</sup> S. Ishida, S. Asano, and J. Ishida, J. Phys. Soc. Jpn. **55**, 936 (1986).
- <sup>13</sup> A. Subedi, cond-mat , arXiv:1311.2922 (2013).
- <sup>14</sup> D. J. Singh and L. Nordstrom, *Plane waves Pseudopotentials and the LAPW Method, 2nd Edition* (Springer, Berlin, 2006).

- <sup>15</sup> P. Blaha, K. Schwarz, G. Madsen, D. Kvasnicka, and J. Luitz, WIEN2k, An Augmented Plane Wave + Local Orbitals Program for Calculating Crystal Properties (K. Schwarz, Tech. Univ. Wien, Austria) (2001).
- <sup>16</sup> J. P. Perdew, K. Burke, and M. Ernzerhof, Phys. Rev. Lett. **77**, 3865 (1996).
- <sup>17</sup> G. Venturini and B. Malaman, J. Alloys Compd. **235**, 201 (1966).
- <sup>18</sup> I. I. Mazin, M. D. Johannes, L. Boeri, K. Koepernik, and D. J. Singh, Phys. Rev. B **78**, 085104 (2008).
- <sup>19</sup> H. Chen, Y. Ren, Y. Qiu, W. Bao, R. H. Liu, G. Wu, Y. L. Xie, X. F. Wang, Q. Huang, and X. H. Chen, EPL **85**, 17006 (2009).
- <sup>20</sup> H. Fukazawa, T. Saito, Y. Yamada, K. Kondo, M. Hirano, Y. Kohori, K. Kuga, A. Sakai, Y. Matsumoto, S. Nakatsuji, K. Kihou, A. Iyo, C. H. Lee, and H. Eisaki, J. Phys. Soc. Jpn. **80**, SA118 (2011).
- <sup>21</sup> D. J. Singh and M. H. Du, Phys. Rev. Lett. **100**, 237003 (2008).
- <sup>22</sup> D. J. Singh, Phys. Rev. B **79**, 174520 (2009).
- <sup>23</sup> T. Sato, K. Nakayama, Y. Sekiba, P. Richard, Y.-M. Xu, S. Souma, T. Takahashi, G. F. Chen, J. L. Luo, N. L. Wang, and H. Ding, Phys. Rev. Lett. **103**, 047002 (2009).
- <sup>24</sup> F. Bondino, E. Magnano, M. Malvestuto, F. Parmigiani, M. A. McGuire, A. S. Sefat, B. C. Sales, R. Jin, D. Mandrus, E. W. Plummer, D. J. Singh, and N. Mannella, Phys. Rev. Lett. **101**, 267001 (2008).
- <sup>25</sup> T. Moriya, *Spin Fluctuations in Itinerant Electron Magnetism* (Springer, Berlin, 1985).
- <sup>26</sup> I. I. Mazin and D. J. Singh, Phys. Rev. B **69**, 020402 (2004).
- <sup>27</sup> T. M. Rice and M. Sigrist, J. Phys.: Condens. Matter **7**, L643 (1995).
- <sup>28</sup> A. P. Mackenzie and Y. Maeno, Rev. Mod. Phys. **75**, 657 (2003).
- <sup>29</sup> G. M. Luke, Y. Fudamoto, K. M. Kojima, M. I. Larkin, J. Merrin, B. Nachumi, Y. J. Uemura, Y. Maeno, Z. Q. Mao, Y. Mori, H. Nakamura, and M. Sigrist, Nature (London) **394**, 558 (1998).
- <sup>30</sup> J. Xia, Y. Maeno, P. T. Beyersdorf, M. M. Fejer, and A. Kapitulnik, Phys. Rev. Lett. **97**, 167002 (2006).